DOXEPIN AS CORROSION INHIBITOR FOR COPPER IN 3.5 wt. % NaCl SOLUTION

SIMONA VARVARA[a*], ROXANA BOSTAN[a], MARIA POPA[a], LUIZA GAINA[b], FLORIN POPA[c]

ABSTRACT. The effect of 3-(dibenzo[b,e]oxepin-11(6H)-ylidene)-N,N-dimethylpropane-1-amine (doxepin) on the corrosion behaviour of copper in 3.5 wt.% NaCl solution was investigated by electrochemical techniques, SEM-EDX and quantum chemical calculations. Polarization curves indicate that doxepin acts as a mixed-type inhibitor. Impedance data also prove the anticorrosive proprieties of doxepin, due to its adsorption on the copper surface. The inhibition efficiency of doxepin increases with increasing its concentration, reaching a maximum value of 88.8% at 5 mM. SEM-EDX analysis revealed that doxepin is able to prevent the formation of the oxides on the copper surface. Quantum chemical calculations are in agreement with the results obtained by electrochemical measurements.

Keywords: *corrosion, copper, doxepin, electrochemical impedance spectroscopy, polarization curve, SEM-EDX, quantum chemical calculations*

INTRODUCTION

Due to its high electrical and thermal conductivity, mechanical workability, and malleability [1], copper is widely used in a variety of fields, including construction, electronics, piping system, transportation, artworks etc. Although copper has good corrosion resistance, when exposed to aqueous media containing high chloride concentrations (*i.e.* HCl, NaCl), it undergoes severe degradation, leading to important economic losses [2]. Starting from '60s [3] up to now, various organic substances containing heteroatoms (*i.e.* N,

[a] *Department of Cadastre, Civil Engineering and Environmental Engineering, "1 Decembrie 1918" University of Alba Iulia, 15-17 Unirii St., 510009 Alba Iulia, Romania*

[b] *Babeş-Bolyai University, Faculty of Chemistry and Chemical Engineering, 11 Arany Janos St., RO-400028, Cluj-Napoca, Romania*

[c] *Materials Science and Engineering Department, Technical University of Cluj-Napoca, 103-105 Muncii Avenue, 400641, Cluj-Napoca, Romania*

* *Corresponding author: svarvara@uab.ro*

S, or P), π bonds, phenyl rings and/or conjugated double bonds were proved to play an important role in the control and mitigation of copper corrosion. Some recent papers review the classes of organic inhibitors for copper corrosion [4, 5], drawing attention to the possibility of using pharmaceutical compounds [5] for effective protection of copper-based materials against corrosion. According to Geethamani and Kasthuri [6], this area of research is important because the expired pharmaceutical drugs are inexpensive, readily available [7] and, in some cases, ecologically acceptable. A literature survey reveals that the levetiracetam [8], ibuprofen [9], metronidazole [10], itraconazole [11], montelukast sodium [12], myclobutanil and hexaconazole [13] and various antibiotics [14-16] have been studied as promising inhibitors for copper corrosion. The inhibition action of these drugs was attributed to blocking the surface *via* the formation of copper complexes on the metallic surface.

The aim of the present paper is to study the inhibiting properties of doxepin drug on copper corrosion in 3.5% wt. NaCl solution. Doxepin is a medication used to treat depressive and anxiety disorders, chronic hives, and trouble sleeping. Potentiodynamic polarization, electrochemical impedance spectroscopy, and scanning electron microscopy coupled with energy dispersive X-ray spectrometry (SEM-EDX) were the main investigation methods. Molecular parameters of doxepin were determined by quantum chemical computations.

RESULTS AND DISCUSSION

Potentiodynamic polarization measurements

Figure 1 shows the cathodic and anodic polarization scans recorded for copper in 3.5% NaCl solution, in the absence and presence of various concentrations of DOX.
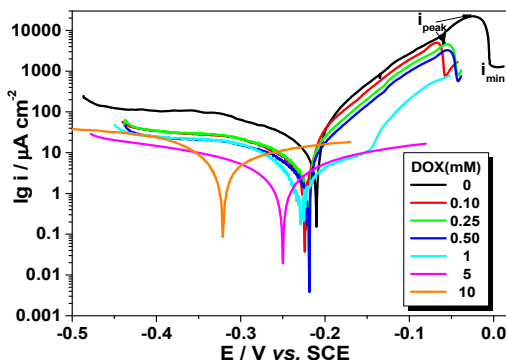

Figure 1. Tafel polarization curves for copper in NaCl 3.5% solution, in the absence and presence of different concentrations of DOX

The anodic behaviour of copper in NaCl solution is well described in the literature [17-20]: first, due to the oxidation of Cu to Cu^+, the current density increases continuously to the peak value (i_{peak}). Then, under the attack of the aggressive Cl^- ions, Cu^+ is rapidly transformed in an insoluble film of CuCl, which leads to a decrease of the current density from i_{peak} to the minimal value (i_{min}). Finally, due to the poor stability of the passive film, CuCl is transformed into soluble cuprous complex $CuCl_2^-$ and the current density starts increasing again. As illustrated in Fig. 1, a small passivation domain could be noticed on the polarization curves obtained in the absence and in the presence of low concentrations of DOX (< 1mM). The addition of the inhibitor, even in low concentrations, decreases the passivation current densities with respect to the blank NaCl solution. However, the anodic current peak disappears, and broad current plateaus are visible in the presence of higher concentrations of DOX (> 1 mM). It should be noted that the anodic dissolution of copper in 3.5 % NaCl solutions containing high concentrations of DOX does not obey the Tafel's law.

As depicted in Fig. 1, both anodic and cathodic current densities decrease with the addition of doxepin as compared to the blank solution. The reducing trend of the current density values is more pronounced as the concentration of the inhibitor increases. A negative shift of the corrosion potentials could be also noticed in the presence of increasing DOX concentrations. These results suggest that doxepin is able to slow down the kinetics of both the anodic dissolution of copper and cathodic oxygen reduction, acting as a mixed-type inhibitor. The anticorrosive properties of doxepin may be related to its adsorption on the copper surface and the formation of a barrier film, impeding the cathodic and the anodic sites, as well.

The values of corrosion parameters, such as the corrosion potential (E_{corr}) and the corrosion current density (i_{corr}) obtained from the polarization curves are summarized in Table 1.

Table 1. Corrosion parameters obtained from the polarization curves of copper in 3.5% NaCl solution, in the absence and in the presence of different concentrations of DOX

DOX (mM)	E_{corr} (mV *vs.* ESC)	i_{corr} ($\mu A\ cm^{-2}$)	IE (%)
0	-165.3	24.10	-
0.10	-223.9	12.56	47.9
0.25	-219.1	7.92	67.1
0.50	-219.2	7.73	67.9
1	-228.5	3.92	83.7
5	-250.2	2.77	88.5
10	-320.8	16.42	65.3

The values of inhibition efficiency (IE), also presented in Table 1, were calculated according to the following equation:

$$IE = \frac{i_{corr}^0 - i_{corr}}{i_{corr}^0} \times 100 \qquad [\%] \qquad (1)$$

where i_{corr}^0 and i_{corr} are the values of the corrosion current densities in absence and in presence of DOX, respectively.

As shown in Table 1, the values of the corrosion current density, i_{corr} decrease with increasing doxepin concentration up to 5 mM. At higher concentrations of inhibitor, a slight increase of the i_{corr} value could be noticed in Table 1, but it remains lower with respect to the blank solution. These results confirm the ability of doxepin to retard the copper corrosion process.

At low concentrations, doxepin exhibits rather a moderate anticorrosive effect on the copper, but the IE values gradually increase with the inhibitor concentration and attain the maximum value of 88.5 % in the presence of 5 mM DOX. A further increase in the DOX concentration to 10 mM leads to a decrease of the IE value at 65.3 %.

Electrochemical impedance spectroscopy

Figure 2 presents the Nyquist diagrams for copper corrosion after 1-h immersion in 3.5% NaCl solution, in the absence and in the presence of various concentrations of doxepin.
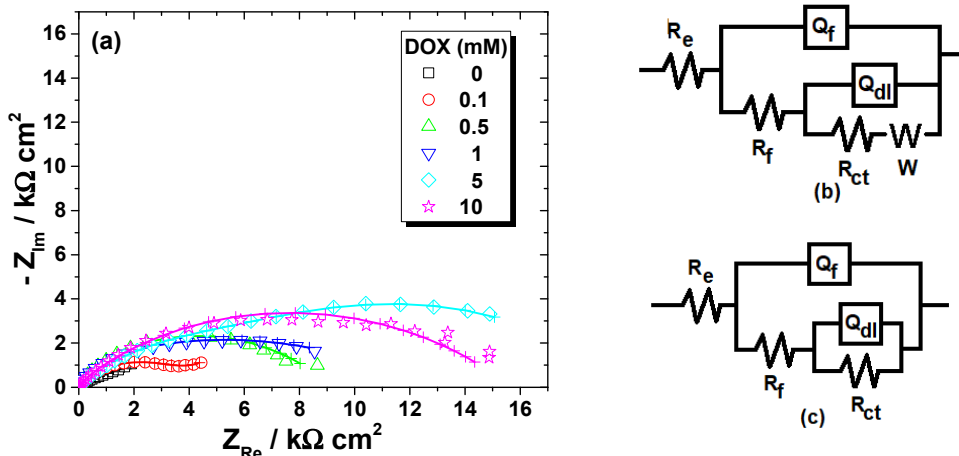

Figure 2. Nyquist diagrams recorded for copper after 1-h immersion in 3.5% NaCl solution, in the absence and in the presence of various concentrations of DOX (a). The equivalent electrical circuits used to fit the EIS data (b, c). Symbols represent the experimental data and lines with cross (—+—) correspond to the simulated spectra.

For the blank solution and in the presence of low concentrations of DOX (< 0.5 mM), a capacitive behaviour could be noticed in high and medium frequency region, followed by a straight line at the low frequency, which might be due to the diffusion of the corrosion reactants and products towards or away from the copper surface [21]. In these cases, the corrosion process is mixed-controlled by the charge-transfer and the diffusion. Although not clearly seen in Figure 2a, two-time constants and a Warburg impedance are necessary to suitably reproduce the experimental data obtained in 3.5% NaCl solution without and with the addition of low concentrations of DOX. Therefore, the corresponding EIS data were interpreted in terms of the equivalent electric circuit depicted in Figure 2b.

As the concentration of DOX increases, the Warburg impedance disappears, and a capacitive behaviour could be noticed over the whole frequency range. The attempts to represent the EIS data of copper exposed to 3.5% NaCl solution containing higher concentrations of DOX ($\geq$ 0.5 mM) by one-time constant circuit did not allow a satisfactory agreement between the model and experimental results. Thus, two-time constants were used for these data simulation, according to the equivalent electrical circuit from Figure 2c.

In the equivalent circuits from Figure 2, R_e represents the electrolyte resistance, the high-frequency parameters, $R_f - Q_f$ correspond to the corrosion product film/inhibitor film [22], while the parameters, $R_{ct} - Q_{dl}$ are attributed to the charge transfer resistance and double layer capacitance. W stands for the Warburg impedance.

As illustrated in Figure 2, the used equivalent electrical circuits reproduce properly the experimental impedance, since a good overlapping between the measured and calculated data was obtained.

The capacitive contributions of the impedance plots were simulated using constant phase elements, represented by the terms Q and n instead of pure capacitors, due to the non-ideal behaviour of the metal surface. The semicircle depression is often explained by the heterogeneity of the surface, caused by roughness, inhibitor adsorption, porous layers formation, the presence of impurities [23].

The impedance of CPE is given by [24]:

$$Q = Z_{CPE(\omega)} = [C(j\omega)^n]^{-1} \tag{2}$$

where Q represents a pre-exponential factor, which is a frequency-independent parameter with dimensions of Ω^{-1} cm^{-2} s^n; j is an imaginary number; $\omega = 2\pi f$ is the angular frequency in rad·s^{-1}; n is the exponent which defines the character of frequency-dependence (-1 $\leq n \leq$ 1).

The values of the pseudo-capacitances (C) associated with constant phase elements were recalculated using the equation:

$$C = \left(R^{1-n}Q\right)^{1/n} \tag{3}$$

The R-Q electrochemical parameters obtained by the fitting procedure are given in Table 2.

The inhibition efficiency (IE) was calculated from EIS measurements according to the following equation:

$$IE(\%) = \frac{R_{ct} - R_{ct}^0}{R_{ct}} x100 \tag{4}$$

where R_{ct} and R_{ct}^0 are the values of the charge transfer resistance, in presence and in absence of DOX, respectively.

Table 2. Electrochemical parameters of copper corrosion in 3.5 wt% NaCl solution obtained in the absence and in the presence of different concentrations of doxepin

DOX (mM)	R_f (kΩ cm²)	Q_f (µF s^{n-1} cm^{-2})	n_f	C_f (µF cm^{-2})	R_{ct} (kΩ cm²)	Q_{dl} (µF s^{n-1} cm^{-2})	n_{dl}	C_{dl} (µF cm^{-2})	W (Ω^{-1} cm^{-2} s$^{1/2}$)	IE (%)
0	0.1	144.8	0.80	51.4	2.2	807	0.51	1400	0.0026	-
0.1	0.5	34.7	0.86	17.5	3.6	1438	0.57	87.4	0.0065	38.9
0.5	0.7	30.2	0.87	16.9	8.5	93.8	0.51	76.1	-	74.1
1	1.0	31.5	0.84	16.2	11.6	80.0	0.50	74.2	-	81.0
5	1.5	11.9	0.70	2.1	19.7	53.8	0.40	58.5	-	88.8
10	0.6	1.7	0.87	0.60	8.4	31.1	0.52	8.8	-	73.8

As could be noticed in Table 2, the film capacitance, C_f values decrease, while simultaneously the film resistances, R_f increase, as the inhibitor concentration increases up to 5 mM. These results suggest that the protective surface film formed in the presence of DOX becomes progressively thicker and less permeable to the aggressive Cl$^-$ ions from the solution.

The charge-transfer resistance, R_{ct} presents larger values in the presence of DOX, confirming its inhibiting effect on copper corrosion, most likely due to the inhibitor absorption on the metallic surface. The decrease of the C_{dl} values in the presence of DOX as compared to its absence could be due to a smaller exposed surface area and/or to a decrease in the local dielectric constant, from which it can be assumed that the water molecules

are gradually replaced by the adsorbed inhibitor molecules [25]. As a result, the inhibition efficiency increases with increasing the doxepin concentration and reaches the highest value of 88.8 % at 5 mM DOX. The decrease of the IE value at higher concentrations of inhibitor (*i.e. 10* mM), agrees with the outcomes of the potentiodynamic polarization measurements. Similar results were previously reported for other inhibitors [26-29] and were attributed to the deterioration or dissolution of the adsorbed layer on the copper surface.

Surface characterization

SEM micrographs and the corresponding EDS spectra of the copper specimens after 24 h of immersion in 3.5% NaCl solution in the absence and in the presence of 5mM DOX are shown in Figure 3.
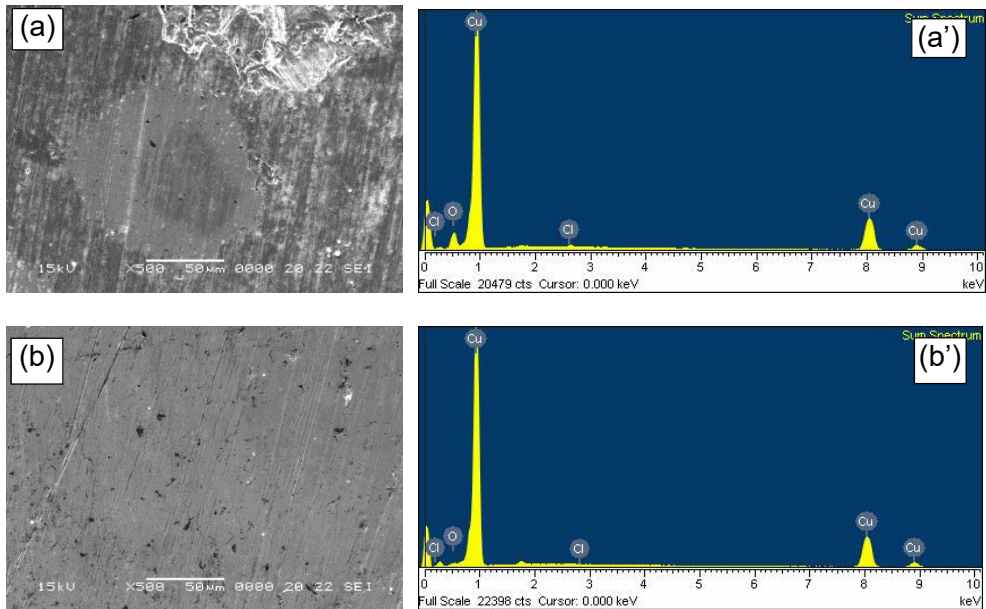
Figure 3. SEM micrographs and EDX spectra of the copper surface after 24 h exposure to 3.5% NaCl solution in absence (a, a') and presence of 5mM DOX (b, b')

In the absence of DOX, the SEM micrograph reveals a severe attack of the copper surface by the aggressive Cl⁻ ions from the electrolyte (Figure 3a). The EDX spectrum reported in Figure 3a' shows the characteristic peaks of copper and a marked presence of the oxygen atoms, together with the chloride atoms.

In the presence of DOX, the copper dissolution process was significantly retarded, and almost no corrosion products are visible on the metallic surface (Figure 3b). Moreover, the amount of oxygen on the copper surface is markedly reduced, as revealed in Figure 3b', confirming that the doxepin adsorption prevents to some extent the formation of oxides on the copper surface.

Quantum chemical calculation

For better understanding the inhibition mechanism of doxepin on copper, quantum chemical calculations and molecule geometry optimization were performed using Spartan'06, followed by semi-empirical (PM3) and 6–31G(d) B3LYP DFT. The generated lowest energy conformers were further used in order to calculate the quantum molecular parameters, such as E_{HOMO}, E_{LUMO}, energy gap, ΔE (E_{HOMO}-E_{LUMO}) and the dipole moment, both in vacuum and water (Table 3).

It is well known that copper is a d type transition metal, characterized by a pronounced tendency to form coordination complexes with donor molecules. It was supposed that the inhibition process is based on the formation of an insoluble and highly adherent donor–acceptor (DA) complex between doxepin and copper. The formation of DA complex involves the electron donation from the HOMO orbitals of doxepin into the vacant copper orbitals, accompanied by backdonation from the metal to the LUMO orbitals of the inhibitor.
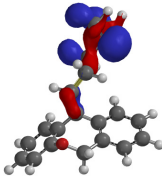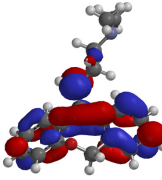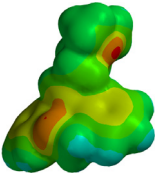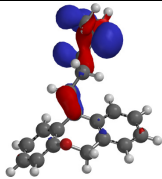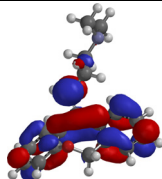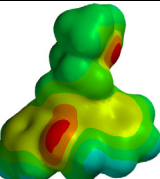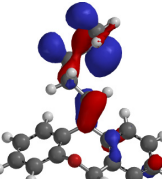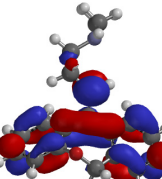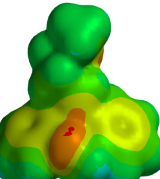
The examination of the frontier molecular orbitals for both isomers E, Z of Doxepin (Table 3) reveals that HOMO orbital overlays the alkene chain preponderantly on the amino group, while LUMO orbital covers the heteroaromatic ring.

Based on the theoretical calculation, it was assumed that the nitrogen atom of doxepin is mainly involved in the electron donation to copper unoccupied orbitals.

CONCLUSIONS

The inhibiting behaviour of 3-(dibenzo[*b,e*]oxepin-11(6H)-ylidene)-N,N-dimethylpropane-1-amine (doxepin) on copper corrosion in 3.5 wt.% NaCl solution was investigated using electrochemical methods (potentiodynamic polarization and electrochemical impedance spectroscopy) surface analysis (SEM-EDX) and quantum chemical calculations. Based on the obtained results, the following conclusions may be drawn:

Table 3. Calculated quantum chemical parameters, repartition of HOMO, LUMO and electrostatic potential map of (E)-3-(dibenzo[b,e]oxepin-11(6H)-ylidene)-N,N-dimethylpropane-1-amine (a. vacuum; b. water) and (Z)-3-(dibenzo[b,e]oxepin-11(6H)-ylidene)-N,N-dimethylpropane-1-amine (c. vacuum)

E [au]	E_HOMO [eV]	E_LUMO [eV]	Dipole [Debye]	HOMO	LUMO	Electrostatic potential map
-866.604337[a]	-5.71[a]	-0.63[a]	1.01[a]			
	ΔE [eV]					
	5.08[a]			a	a	a
-866.616426[b]	-5.99[b]	0.80[b]	1.30[b]			
	ΔE [eV]					
	5.19[b]			b	b	b
-866.606396[c]	-5.73[c]	-0.57[c]	1.08[c]			
	ΔE [eV]					
	5.06[c]			c	c	c

(1) Doxepin presents inhibiting properties for copper corrosion in NaCl solution; its inhibition efficiency increases with increasing the drug concentration up to an optimum value of 5 mM.

(2) Polarization curves indicate that doxepin acts as a mixed-type inhibitor.

(3) Impedance data revealed the anticorrosive proprieties of doxepin, most likely due to its adsorption on the copper surface, as proved by the decrease of the double layer capacitance in presence of DOX.

(4) SEM-EDX analysis showed that doxepin is able to prevent to some extent the corrosion products formed on the copper surface.

(5) Quantum chemical calculations agree with the results obtained by electrochemical measurements.

EXPERIMENTAL SECTION

The corrosive blank solution containing 3.5 wt.% NaCl was prepared by dissolving the analytical grade NaCl (Merck, Germany) in distilled water.

For the corrosion studies, tablets of 25 mg doxepin (DOX) purchased from a local drug store were used. The active substance from doxepin is 3-(dibenzo[*b,e*]oxepin-11(6H)-ylidene)-N,N-dimethylpropane-1-amine).

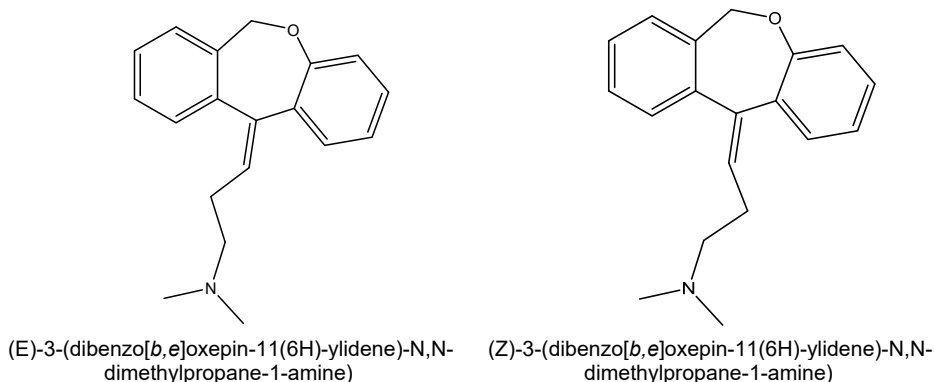The molecular structures of the two isomers of doxepin are presented in Figure 4.

(E)-3-(dibenzo[*b,e*]oxepin-11(6H)-ylidene)-N,N-dimethylpropane-1-amine)   (Z)-3-(dibenzo[*b,e*]oxepin-11(6H)-ylidene)-N,N-dimethylpropane-1-amine)

Figure 4. Molecular structure of the two isomers of 3-(dibenzo[*b,e*]oxepin-11(6H)-ylidene)-N,N-dimethylpropane-1-amine)

The drug was dissolved in the 3.5 wt.% NaCl electrolyte, in order to obtain various concentrations of DOX, in the range of 0.1 mM to 10 mM.

The electrochemical investigations were carried out at room temperature using a conventional three-electrode cell. The working electrode was a pure copper disk embedded in epoxy resin, with an exposed surface area of 0.38 cm^2. A saturated calomel electrode (SCE) and a large area platinum electrode were used as reference and counter electrodes, respectively.

Prior to all measurements, the copper electrode was grounded using successive grades of silicon carbide paper up to 4000, washed thoroughly with distilled water and degreased with ethanol.

Electrochemical measurements were carried out using PAR 2273 potentiostat controlled by computer. Polarization measurements were performed after 1-h immersion of the copper electrode in the test solution, at a scan rate of 10 mV/min, in the potential range of ± 200 mV *vs.* open circuit potential.

Electrochemical impedance spectroscopy measurements (EIS) were carried out at open circuit potential, after 1-h immersion of the working electrode in the corrosive solution. The impedance spectra were acquired in the frequency range of 10 kHz to 10 mHz, at 5 points per hertz decade, with an AC voltage amplitude of ± 10 mV. The impedance data were interpreted using ZSimpWin V3.21 software.

For morphological studies, the copper samples were immersed for 24 hours in 100 mL of 3.5 % NaCl solution, in the absence and presence of 5 mM DOX. Then, the copper electrodes were carefully washed with distillated water, dried at room temperature and further analysed by scanning electron microscopy, using a Jeol JEM 5510 LV electron microscope coupled with an EDX analyser (Oxford Instruments, INCA 300).

In an attempt to determine the most stable geometry of the inhibitor molecule, the minimum energy was evaluated starting with molecular mechanics optimization of the conformers generated within the Confanal module of Spartan'06 [30], followed by semi-empirical (PM3) and 6–31G(d) B3LYP DFT calculations [31-33] on all such obtained conformers.

REFERENCES

1. M. Shabani-Nooshabadi; F.S. Hoseiny; Y. Jafari; *Metall. Mater. Trans. A*, **2015**, *46*, 293–299.
2. D.S. Chauhan; M.A. Quraishi; C. Carrière; A. Seyeux; P. Marcus; A. Singh; *J. Mol. Liq.,* **2019**, *289*, 111-113.
3. I. Dugdale; J.B. Cotton; *Corros. Sci.*,**1963**, *3,* 69–74.
4. M.M. Antonijevic; M.B. Petrovic; *Int. J.Electrochem. Sci.*, **2008**, *3*, 1–28.
5. A. Fateh; M. Aliofkhazraei; A.R. Rezvanian; *Arab. J. Chem.*, **2020**, *13*, 481-544.
6. P. Geethamani; P.K. Kasthuri; *J. Taiwan. Inst. Chem. E.*, **2016**, *63*, 490–499.
7. N. Vaszilcsin; V. Ordodi; A.Borza; *Int. J. Pharm.*, **2012**, *431*, 241– 244.
8. G. Karthik; M. Sundaravadivelu; *Egypt. J. Pet.*, **2016**, *25*, 481–493.
9. Z.Z. Tasić; M.B. Petrović Mihajlović; A.T. Simonović; M.B. Radovanović; M.M. Antonijević; *Sci. Rep.*, **2019**, *9*, 1-14.
10. A. Samide; B. Tutunaru; A. Dobriţescu; P. Ilea, A.C. Vladu; C. Tigae; *Int. J. Electrochem. Sci.*, **2016**, *11*, 5520–5534.
11. Z. Gong; S. Peng; X. Huang; L. Gao; *Materials*, **2018**, *11*, 1-17.
12. B. Tan; S. Zhang; Y. Qiang; L. Feng; C. Liao; Y. Xu; S. *Chen; J. Mol. Liq.*, **2017**, *248*, 902–910.
13. W. Li; L. Hu; S. Zhang; B. Hou; *Corros. Sci.*, **2011**, *53*, 735–745.
14. R. Ganapathi Sundaram; G. Vengatesh; M. Sundaravadivelu, *J. Bio. Tribo. Corros.,* **2017**, *36*, 3-13.

15. R. Farahati; S. Morteza Mousavi-Khoshdel; A. Ghaffarinejadb; H. Behzadi; *Prog. Org. Coat.*, **2020**, *142*.
16. G. Gece; *Corros. Sci.*, **2011**, *53*, 3873–3898.
17. G. Kear; B.D. Barker; F.C. Walsh; *Corros. Sci.*, **2004**, *46*, 109–135.
18. A. Shaban; E. Kálmán; J. Telegdi; *Electrochim. Acta.*, **1998**, *43,* 159–163.
19. K.F. Khaled; M.A. Amin; *Corros. Sci.*, **2009,** *51*, 2098–2106.
20. C. Rahal; M. Masmoudi; M. Abdelmouleh; R. Abdelhedi; *Prog. Org. Coat.*, **2015**, *78*, 90–95.
21. Y. Qiang; S. Zhang; S. Yan; X. Zou; S. Chen; *Corros. Sci.*, **2017**, *126,* 295–304.
22. H. Tian; W.Li; K. Cao; B. Hou; *Corros. Sci.*, **2013**, *73*, 281–291.
23. A. Popova; M. Christov; A. Vasilev; *Corros. Sci.*, **2011**, *53*, 1770–1777.
24. I.D. Raistrick; J.R. MacDonald; D.R. Franceschetti; *The electrical analogs of physical and chemical processes. Impedance Spectroscopy Emphasizing Solid Materials and Systems*, John Wiley & Sons, J.R. MacDonald (Ed.), New York, **1987**, pp. 27–84.
25. Y. Qiang; S. Zhang; L. Guo; X. Zheng; B. Xiang; S. Chen; *Corros. Sci.*, **2017**, *119,* 68–78.
26. R. Bostan; S. Varvara; L. Găină; L.M. Mureșan; *Corros. Sci.,* **2012**, *63*, 275–286.
27. S. Varvara; R. Bostan; O. Bobiș; L. Găină; F. Popa; V. Mena; R.M. Souto; *Appl. Surf. Sci.*, **2017**, *426*, 1100–1112.
28. K. Barouni; L. Bazzi; R. Saghi; M. Mihit; B. Hammouti; A. Albourine; S.E. Issami; *Mat. Lett.,* **2008**, *62*, 3325–3327.
29. K.M. Ismail; *Electrochim. Acta.*, **2007**, *52*, 7811–7819.
30. SPARTAN'06 Wavefunction, Inc., Irvine, CA.
31. D.J. Becke; *Chem. Phys.*, **1993**, *98*, 5648–5652.
32. P.J. Stephens; J. Devlin; C.F. Chabulowski; M.J. J Frisch; *Phys. Chem.,***1994**, *98*, 11623–11627.
33. C. Lee; W. Yang; R.G. Parr; *Phys. Rev. B.*, **1988,** *37*, 785–789.